Civil Engineering Infrastructures Journal, 48(2): 305-322, December 2015
ISSN: 2322-2093

Load Test and Model Calibration of a Horizontally Curved Steel Box-Girder Bridge

Rezaie, F. [1*], Ahmadi, G. [2] and Farnam, S.M. [3]

[1] Assitant Professor, Department of Civil Engineering, Bu-Ali Sina University, Hamedan, Iran.

[2] M.Sc., Department of Civil Engineering, Bu-Ali Sina University, Hamedan, Iran.

[3] Ph.D. Candidate, Department of Civil Engineering, Bu-Ali Sina University, Hamedan, Iran.

Received: 02 Jun. 2014 Revised: 11 Jul. 2015 Accepted: 11 Jul. 2015

Abstract: In this paper, full scale load test of a horizontally curved steel box-girder bridge is carried out in order to detect structural defects, which reportedly result in unwanted vibrations in nearby buildings. The bridge is tested under the passage of six heavy vehicles at different speeds, so as to determine its static and dynamic responses. A total number of one hundred and two (102) sensors are used to measure the displacements, strains, and accelerations of different points of the bridge. It is observed that the bridge vibrates at a fundamental frequency of 2.6 Hz intensively and the first mode of vibration is torsional instead of flexural. The dominant frequency of vibration of the nearby buildings is computed to be approximately 2.5Hz using rational formulas. Thus, nearness of the fundamental frequency of the bridge to those of the adjacent buildings may be causing resonance phenomenon. However, in static load tests, low ranges of strain and displacement illustrated adequate structural capacity and appropriate safety under static loads. Numerical models are created using ANSYS and SAP2000 software products, so as to design the loading test and calibrate the finite element models. The connections of the transversal elements to the girders, transversal element spacing, and changes of the stiffness values of the slabs were found to be the most influential issues in the finite elements calibration process. Finally, considering the total damage of all members, the final health score of the bridge was evaluated as 89% indicating that the bridge is in a very good situation.

Keywords: Dynamic and static loading tests, Frequencies of vibration, Horizontally curved bridges, Steel box-girder.

INTRODUCTION

Bridge performance and health monitoring can be carried out using numerical modeling, *in-situ* load testing, or a combination of both. Load testing of bridges is an economical and practical way of understanding structures' behavior, structural health monitoring and aging (Scott et al., 2006). Structural Health Monitoring (SHM) is the process of implementing a damage detection that collects data on a continuous basis (Gomez et al., 2011; Hui et al., 2011). SHM system is the development and characterization of a baseline response that is sensitive to meaningful changes in the structural system, and insensitive to normal operational changes (McCullagh et al., 2014; Yarnold and Moon, 2015). Structural health monitoring was conducted on various bridges such as composite bridges (Kistera et al., 2007; Adewuyi and Wu, 2009). In recent years, the need to maintain and protect critical infrastructural links has led to

* Corresponding author Email: frezaie@gmail.com

significant developments in the area of structural health monitoring. Statistical analyses of sensor data revealed useful information about bridge behavior (Ataeia et al., 2005; Ghorbanpour and Ghassemieh, 2011). Static and dynamic tests presented useful information about the actual behavior of bridges under traffic loads. Since the actual structures are typically complex, obtaining this information analytically is usually difficult. Hence, simplifying assumptions were used to facilitate the process of obtaining this information from the bridge load tests.

The use of curved bridges at intersections of modern highway systems is quite popular, since they allow the congested traffic flow to pass smoothly and are aesthetically pleasing. Box-girders are the most preferred sections for curved bridges on account of their high torsional capacity. Though considerable amount of analytical and experimental work has been undertaken on the dynamics of straight bridges, comparatively little work has been carried out in relation to the behavior of curved bridges (Chang and White, 2008; Naeeni and Fazli, 2011).

In this paper, full scale testing of a horizontally curved steel box-girder bridge is carried out, considering the Ghale Morghi Bridge, Tehran, Iran as the case study (Figure 1). The main objectives could be summarized as:

1. To develop an enhanced understanding of the dynamic response of horizontally curved bridges.
2. To detect structural defects that cause unwanted vibrations to nearby buildings.
3. To conduct a structural health monitoring procedure on the bridge.
4. To calibrate the finite element model comparing the loading test data to that of ANSIS.

Performing a full scale dynamic test on a bridge requires complete closure in order to avoid any unwanted loading. Complete closure is, however, quite difficult as the bridge might serve as a necessary daily road access in urban areas. Highway bridges are subject to dynamic forces imposed by moving vehicles. All moving vehicles generate additional dynamic effects on the bridges (Ilze and Ainars, 2013; Sun et al., 2013).

Having a composite superstructure (steel-concrete), the Ghale Morghi bridge was built in 1995 providing four traffic lanes. Composite bridges were constructed by placing concrete slabs on steel or precast pre-stressed girders with shear connectors to guarantee monolithic behavior (Demetrios and Tonias, 1995). Composite members, consisting of a steel girder and a cast-in-place concrete deck, sensitive to vibration in composite sections, must be considered (Kwak et al., 2000).

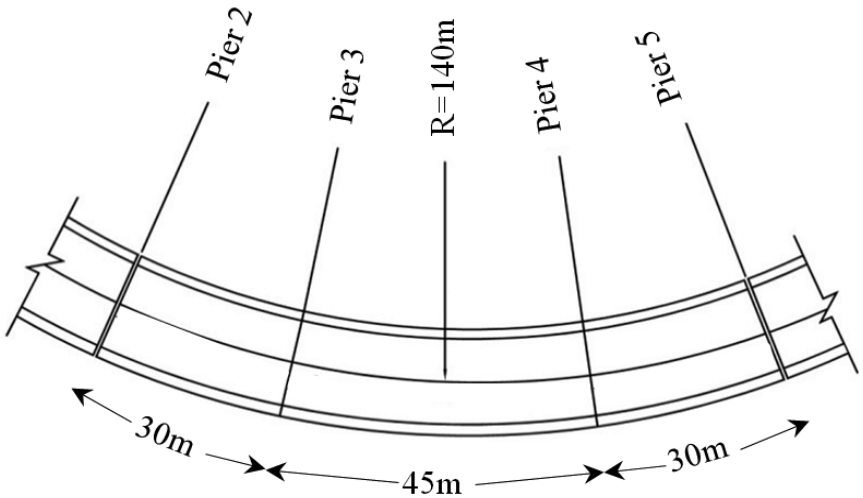

Fig. 1. Plan view of the Ghale Morghi bridge, Tehran, Iran

Bridges with steel beams and concrete decks are very efficient when considering loading capacity and manufacturing/ maintenance costs. This is why these bridges are commonly used in cities and roadways (Montens et al., 2003). However, undesirable vibration under service loads was reported in many cases (Kavatani et al., 2000). Yang et al. (2004) and Yau et al. (2001) separately performed some research on the removal of these undesirable vibrations and suggested the use of expansion joints and elastomer supports. Green and Cebon (1994) in their study investigated some experimental case studies in order to validate numerical and theoretical results.

Bridge Description

The Ghale Morghi bridge is about 225 m long and consists of seven unequal spans broken into three distinct units (Figure 1). These units were separated by expansion joints, which provide hinges in the otherwise continuous structure. The mid-unit is 105 m long with three spans, and the longest span occurs between Piers 3 and 4 and is 45 m long (Figure 2). The bridge is horizontally curved. Figure 2 shows that the radius of curvature for the longest span (Piers 3 to 4) is 140 m.

The superstructure consisted of four curved box-girders made of st-37 steel. Figure 3 shows the measured flange and web dimensions. Center-to-center distance of the box-girders is 4.4 m and the distance from the center of the external box-girder to the edge of the deck is 2.3 m. The bridge slab is nominally a 250 mm thick cast-in-place concrete slab and the average cylindrical strength of the concrete is 30 MPa.

Fig. 2. Access railroad between piers 3 and 4

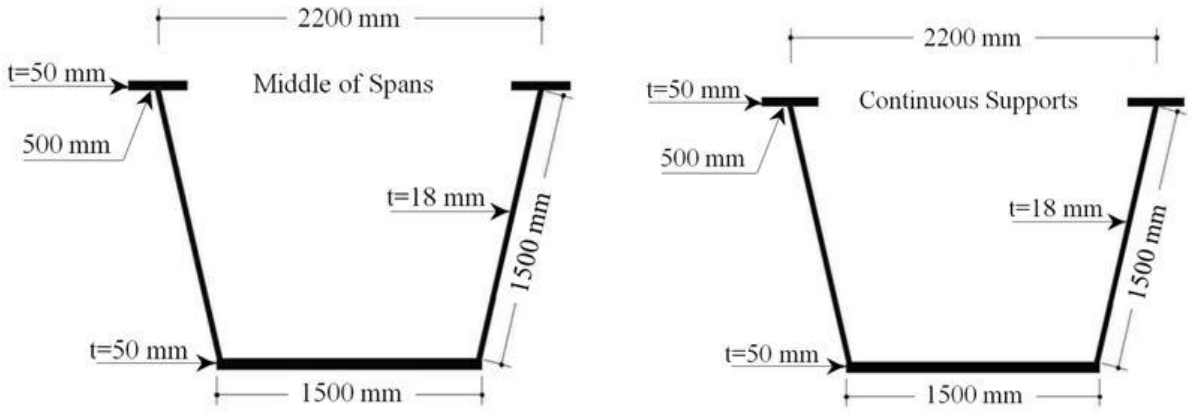

Fig. 3. Box-girder cross-sections in mid-unit

Instrumentation and Data Acquisition

The main focus of this project was placed upon the mid-unit of the bridge between piers 2 and 5. Thus, the three spans of the mid-unit on the railroad are instrumented (Figures 1 and 2). According to the proposed loading program one hundred and two (102) sensors were placed to measure accelerations at 34 points, displacements at 39 points and strains at 29 points. Sensors were installed in the longitudinal direction at three sections on the supports (S1, S3, and S5) and two sections in the mid-spans (S2 and S4), as shown in Figure 4. Figure 5 shows the box-girder numbering and LVDT positions in a typical section. Installed sensors were connected to terminals supporting ninety-eight (98) static and forty-eight (48) dynamic channels.

The coding scheme used for the sensors consisted of six characters. The first character designated the type of sensor, i.e. 'A' for accelerometer gauges, 'S' for strain gauges and 'D' for displacement transducers (LVDT). The second character identified the label of the selected section (1 to 5), as shown in Figure 4. The third character 'B' in combination with digits 1 to 4 (fourth character) denotes the longitudinal box-girder to which the sensor was placed. The characters that can take the fifth position are divided into two groups. Characters 'T' and 'B' identified the strain gauges placed on the top or bottom of the girder while characters 'V' and 'L' determined the vertical and lateral component of displacement or acceleration gauges. The sixth character 'E' or 'I' designates the exterior or interior side of the box-girder.

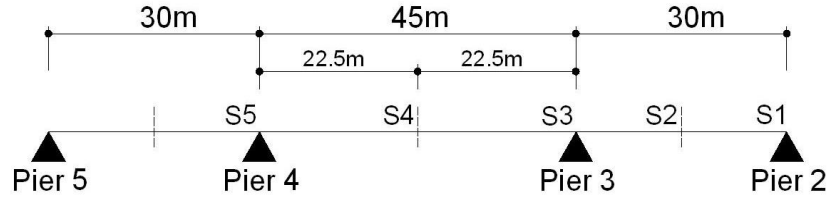

Fig. 4. Selected sections (S1 to S5) for installing sensors in the longitudinal direction

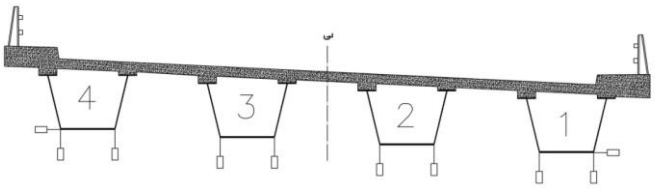

(a)

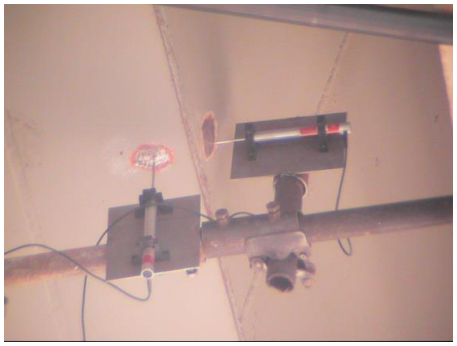

(b)

Fig. 5. a) Box-girder numbering and LVDT positions in a typical section, b) Displacement transducers installed on the first box-girder (the interior box-girder)

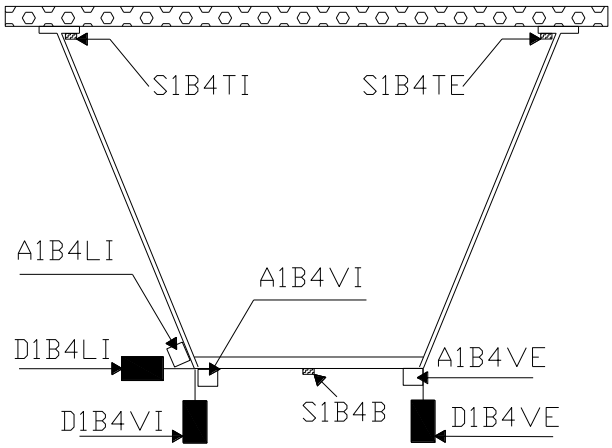

Fig. 6. Positions and coding schemes of the sensors

TEST LOADING

Test Vehicle

A three-axle vehicle with a gross mass of 27 tones and maximum wheel base of 4 m was used as a test vehicle. During the test, six vehicles were used. These vehicles have a short wheel base and a considerable mass to induce an adequate output response in the bridge. The vehicle load details are shown in Figure 7.

Testing Procedure

Six different programs were considered for the testing procedure. These programs include influence line, harmonic loading, static bending, static torsion, dynamic bending and dynamic torsion tests (Standard Loads for Bridges, 2000). In the influence line test, each of the lanes was loaded by a vehicle, which travelled at a constant velocity of 5 km/h. Strains, displacements and accelerations were recorded for all runs using the data acquisition system at established increments. In the harmonic test, lane 4 was loaded by a train of six vehicles traveling at a constant velocity of 20 km/h and 15 m distance. In this program, the behavior of the structure was investigated under harmonic loading with a period of 3.8 s (Figure 8).

In the static bending test, lanes 1 to 4 were loaded by placing the second axle of vehicles on the radius passing through the middle of third, fourth and fifth spans and on the radius passing through the quarter length of the fourth span (Figure 9). In the static torsion test, vehicles were placed rear to rear on lanes 3 and 4 such that the radius passing through the middle of spans 3, 4 and 5 lies between the vehicles (Figure 8).

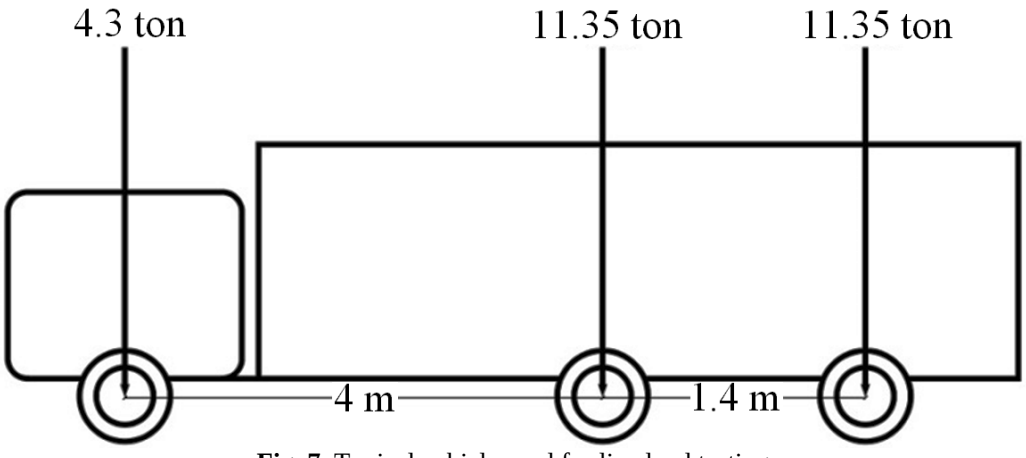

Fig. 7. Typical vehicle used for live load testing

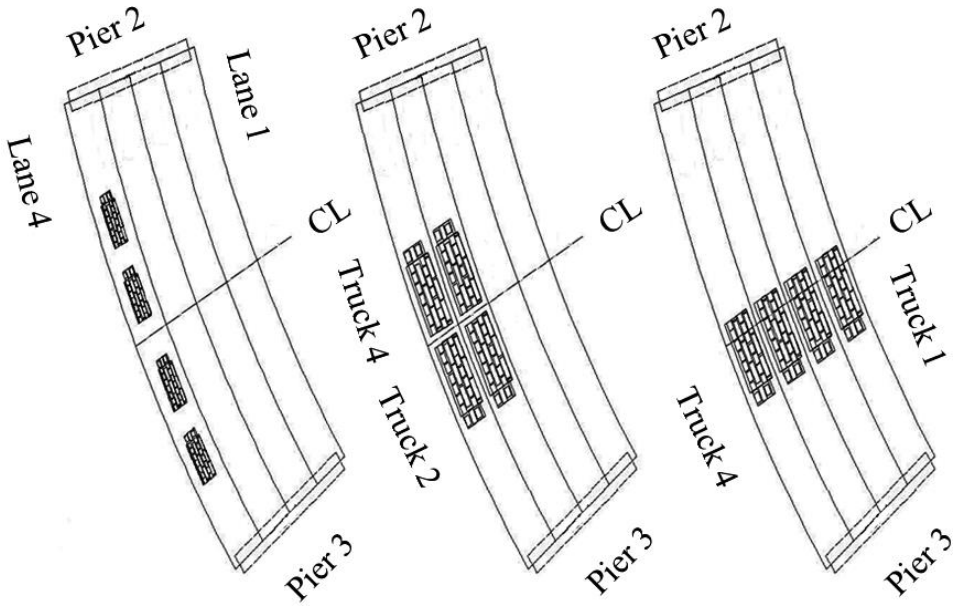

Fig. 8. Arrangement of test vehicles in a) harmonic, b) torsion and c) bending static–dynamic tests

Fig. 9. Test vehicles used for static bending test

In dynamic bending test, four vehicles were made to pass through lanes 1 to 4 in the same direction at a constant velocity of 20 km/h. In this loading program, the aim was to evaluate the bending behavior of the superstructure under dynamic loading (Figure 9). In the dynamic torsion test, four vehicles were made to pass through lanes 3 and 4 at a constant velocity of 20 km/h (Figure 8).

NUMERICAL STUDY

Primal Numerical Model

In order to assess the structure of the bridge, six loading programs were proposed using specified vehicles. These loading programs were created with the primal approximate numerical model after controlling critical sections of moment and shear in SAP2000 (Figure 10). These tests are divided into static and dynamic loading programs that are intended to evaluate the behavior of the bridge structure.

Numerical Model

The next step is to build a 3-D numerical model of the structure using ANSYS software (Figure 11). The first SAP2000 model was built and the results were inaccurate. Then, the model was calibrated with loading test results on a trial and error

process. Material properties and boundary conditions were regulated during the calibration process (Mohammad et al., 2004; Darius et al., 2013). Bending stiffness of supports, transversal elements connections to the box-girder and the slab stiffness changes were considered to be the calibration parameters of the model and, finally, its behavior matched that of the actual structure. Then, the mathematical model was used to check the behavior under any type of loading. In order to find out how close the results of the numerical modeling could be to those of the loading tests, several three-dimensional models of the bridge with different levels of accuracy were made. It is not possible to create very detailed models, because parts of the structure are out of reach and some gusset plates could not be modeled. Therefore, it is quite expectable that the dominant frequency of vibration of bridge structure obtained from models (2.1 Hz) does not completely agree with the results of loading tests (2.6 Hz). However, the difference of the values is acceptable within the accuracy of the models.

It is worth mentioning that unlike straight bridges for which the first mode of vibration is flexural (AASHTO Standard Specification for Highway Bridges, 2002), for this specific bridge, the first mode of vibration is torsional (Figure 12). This behavior can be attributed to the great difference between outer and inner length and stiffness of the bridge superstructure (AASHTO Guide Specifications for Horizontally Curved Steel Girder Highway Bridges with Design Examples for I-Girder and Box-Girder Bridges- American Association of State and Highway Transportation Officials, 2003).

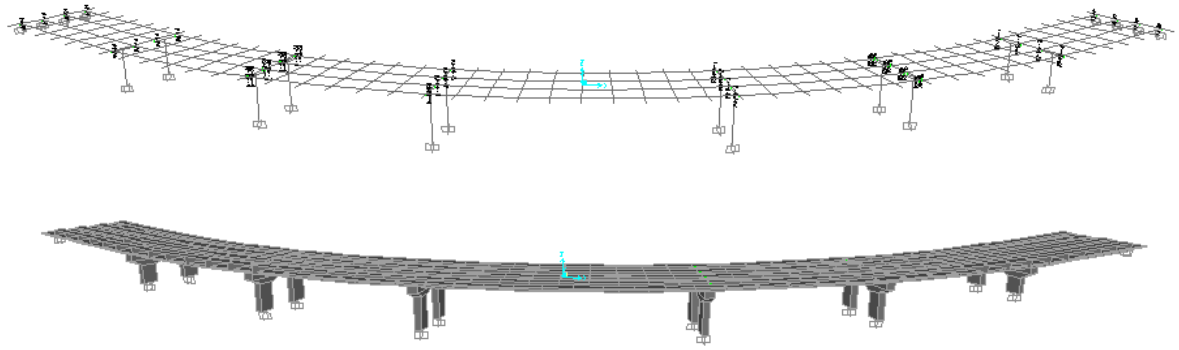

Fig. 10. FEM model of the Ghale Morghi bridge

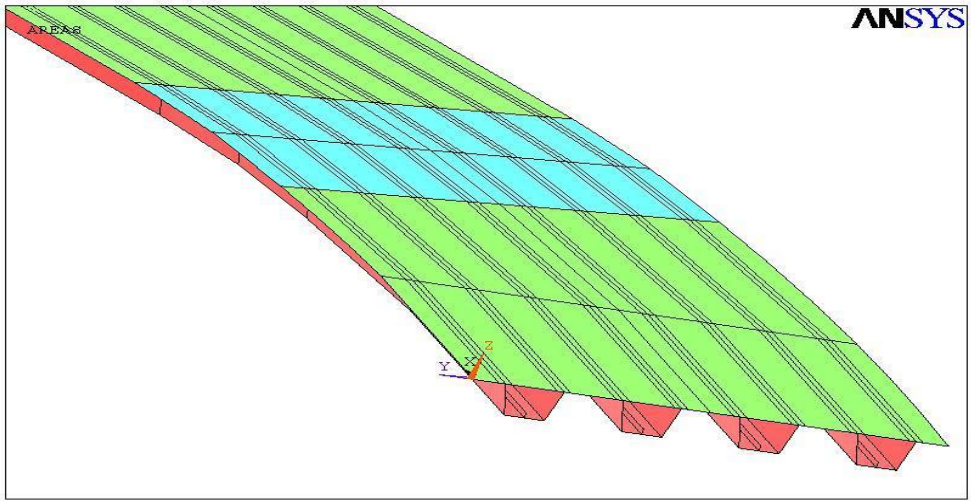

Fig. 11. Isometric perspective numerical 3-D model

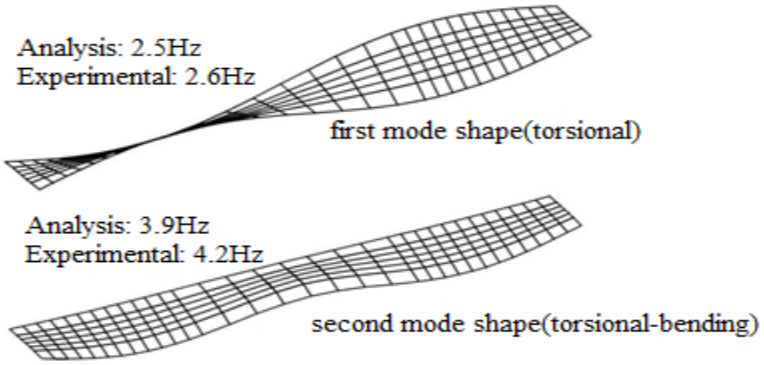

Fig. 12. First and second vibration mode shape of the bridge

TEST RESULTS

Results of Static Test

After balancing all the gauges and establishing initial zeros, the bridge was subjected to the test vehicles. Strain gauge results showed that the maximum strain was limited to 100 micro strains in the beams (Figure 13). Due to the linear relationship between stress and strain, maximum stress under static bending and torsion test was limited to 10MPa.

In sections 2 and 4 due to the vehicles' different locations (Fig. 4), static test and calibrated FEM analysis results for displacements are presented in Tables 1, 2 and 3. It is evident that the low ranges of strains and displacements in static load test indicate adequate structural capacity and appropriate safety under static loads.

Results of the Dynamic Test

A total number of 44 acceleration gauges were installed at different places of the bridge to record the response of the structure when a 28 ton vehicle passes through the fourth lane at a velocity of 50 km/h. The response includes the results of Fast Fourier Transform for vertical acceleration gauges at sections 1, 3 and 4 and Fast Fourier Transform for ground vibration in three mutual directions. These results are shown graphically (Figures 14-17).

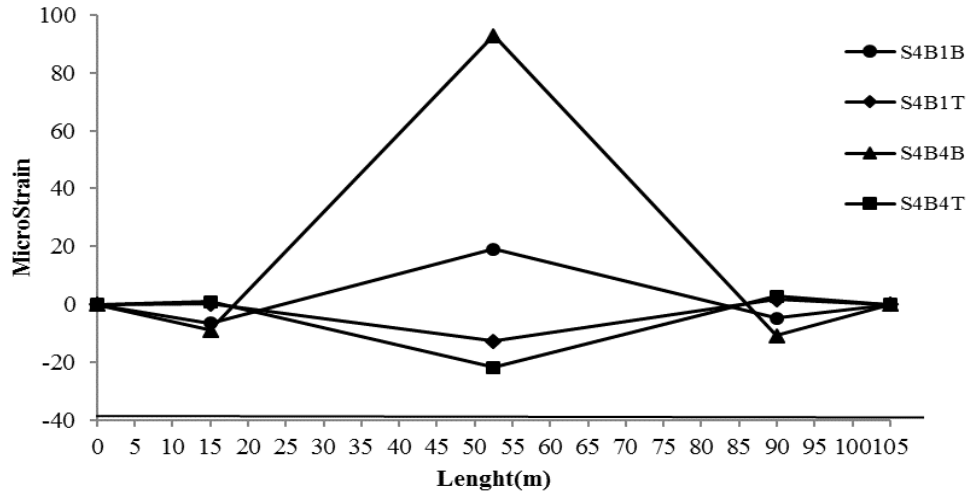

Fig. 13. Top flange strain in 1&4 box-girder due to vehicle location in static torsion test

Table 1. Displacement value in the middle of the 3rd span (section 2) due to vehicle locations loading test

Static torsion test (mm)			Static bending test (mm)					Sensor
S2	S4	S6	S6	S4-5	S4	S3-4	S2	
-1.36	1.73	-0.39	-0.46	1.33	2.31	2.40	-4.53	D2B1VI
-4.01	2.74	-0.54	-0.54	1.56	2.70	2.80	-5.16	D2B2VI
-6.95	3.80	-0.69	-0.63	1.82	3.09	3.20	-5.77	D2B3VI
-9.93	4.93	-0.85	-0.72	2.05	3.51	3.63	-6.46	D2B4VI

Table 2. Displacement value in the middle of the 3rd span (section 2) due to vehicle locations FEM analysis

Static torsion analysis (mm)			Static bending analysis (mm)					Sensor
S2	S4	S6	S6	S4-5	S4	S3-4	S2	
-1.19	1.66	-0.29	-0.29	1.23	2.2	2.12	-4.12	D2B1VI
-3.21	2.32	-0.42	-0.40	1.35	2.49	2.35	-5.57	D2B2VI
-7.95	3.28	-0.56	-0.42	1.55	2.85	2.72	-6.14	D2B3VI
-8.84	3.99	-0.66	-0.50	1.63	3.06	2.92	-5.80	D2B4VI

Table 3. Displacement value in the middle of the 4rd span (section 4) due to vehicle locations loading test

Static torsion test (mm)			Static bending test (mm)					Sensor
S2	S4	S6	S6	S4-5	S4	S3-4	S2	
1.63	-4.30	1.63	2.40	-6.77	-10.19	-6.77	2.40	D4B1VI
4.66	-22.3	4.66	3.62	-9.73	-14.66	-9.73	3.62	D4B4VI

Table 4. Displacement value in the middle of the 4rd span (section 4) due to vehicle locations FEM analysis

Static torsion analysis (mm)			Static bending analysis (mm)					Sensor
S2	S4	S6	S6	S4-5	S4	S3-4	S2	
1.56	-4.48	1.49	2.01	-5.47	-8.69	-5.55	2.22	D4B1VI
3.63	-16.86	3.58	2.67	-7.18	-11.72	-7.42	2.92	D4B4VI

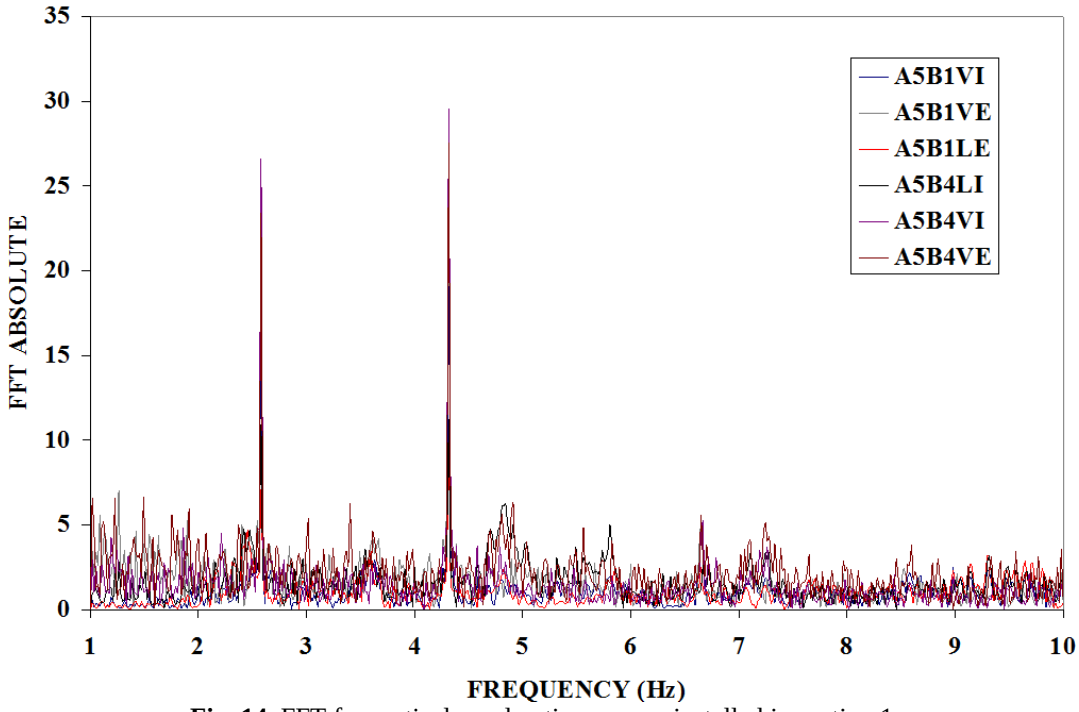

Fig. 14. FFT for vertical acceleration gauges installed in section 1

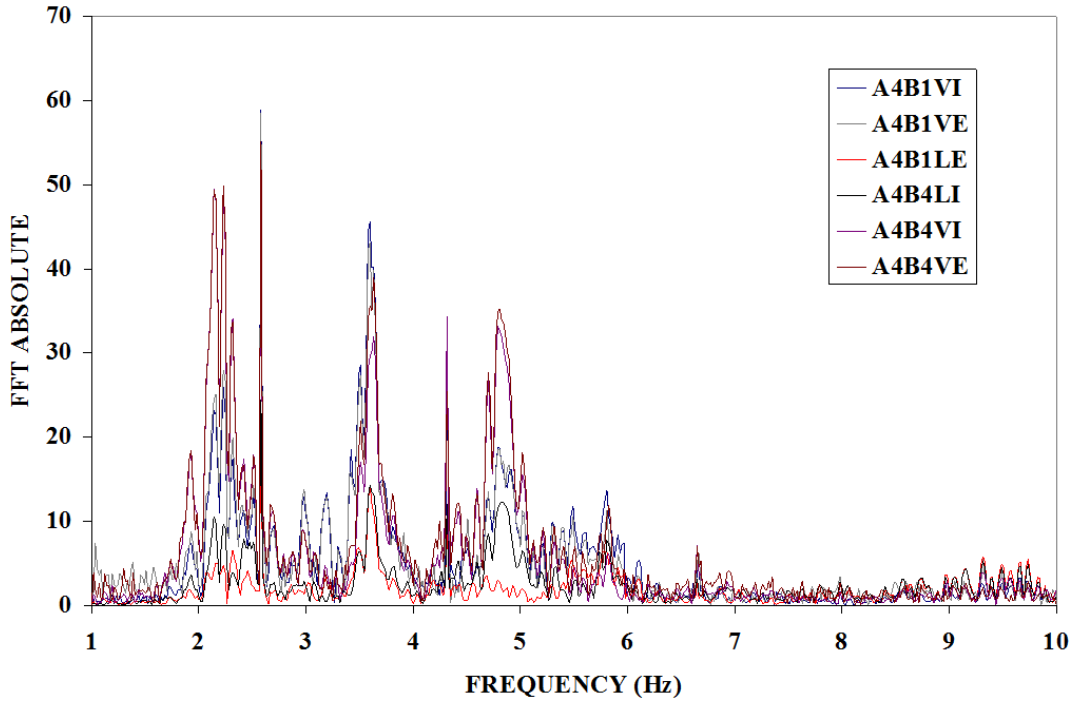

Fig. 15. FFT for vertical acceleration gauges installed in section 4

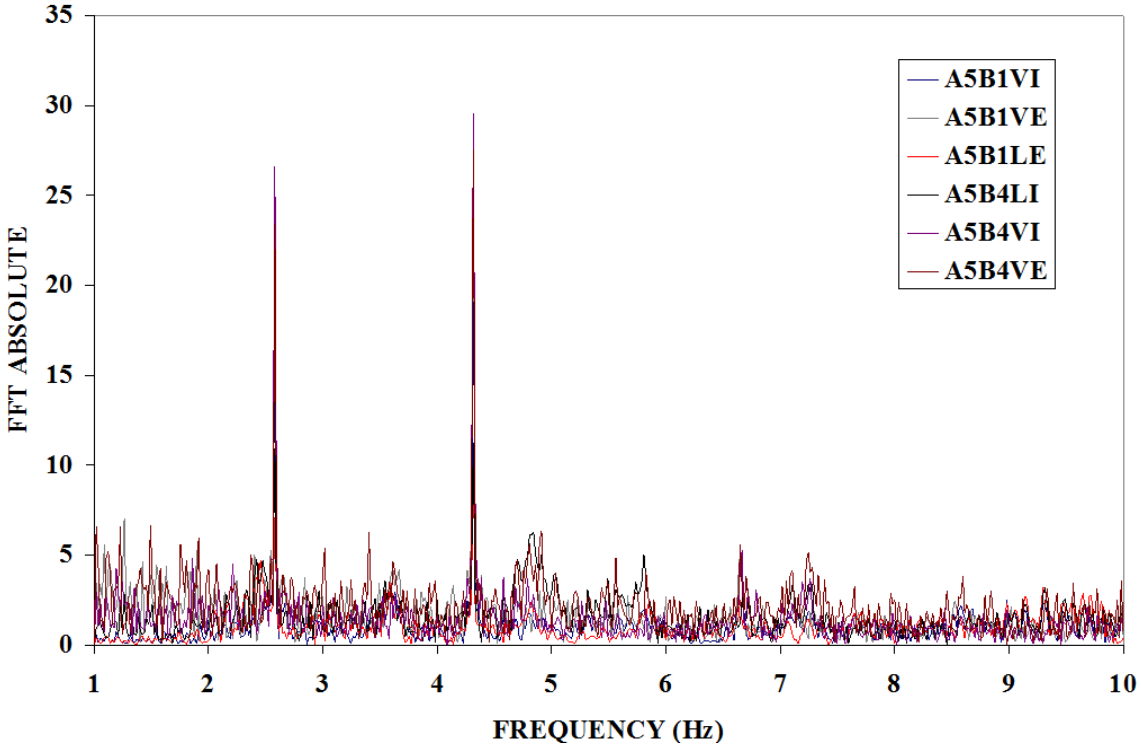

Fig. 16. FFT for vertical acceleration gauges installed in section 5

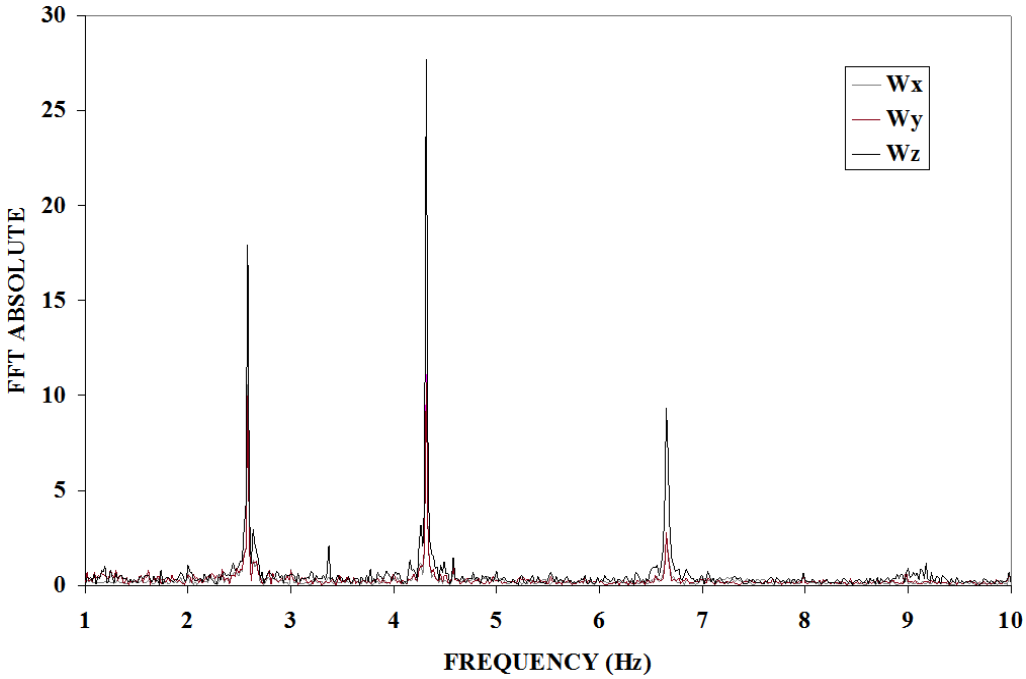

Fig. 17. FFT for vertical (W_z) and horizontal (W_y) acceleration gauges on ground

The bridge has unequal span lengths and closely spaced natural frequencies. Figures 14- 17 show the bridge structure experiences sever vibrations at frequencies 2.6 and 4.2Hz respectively. Dominant frequency of vibration of nearby buildings was computed using rational formulas to be approximately 2.5Hz. Thus, the proximity of the fundamental frequency of the bridge with that of the surrounding buildings might cause resonance phenomenon.

MODEL CALIBRATION

Calibration of the finite element model of the bridge is the process of modifying the input parameters until the output of the numerical model matches a set of obtained data. The calibrated FE model has a good correlation with the static and dynamic measurements and is used for continuous structural health monitoring of the bridge (Wang et al., 2010). The sole purpose of model calibration is to improve the uncertain model parameters or imprecise modeling assumptions such that the FE model predictions are closer representations of reality (Sevim et al., 2011). The efficiencies of the cases below were studied in the Ghale Morghi Bridge finite element model for calibration:

1. Transversal element connection to girder.
2. Transversal element spacing.
3. Slab stiffness changes.

Transversal Element to Girder Connection

In static torsion test, displacements of B1 and B4 middle span are shown in Figure 18 for two connections. Displacements of rigid and fixed connections were studied and compared with the test results. Vehicles were placed in the middle of these spans with 5 m transversal element spacing.

The vertical displacements of these beams with rigid connection have better result as compared to fixed connection (Figure 18).

Transversal Element Spacing

The effect of transversal element spacing on the displacement of the fourth middle span is shown for four different values: 0.5, 1.25, 2.5 and 5 m (Figure 19). Transversal element to girder connection is supposed to be rigid in this diagram.

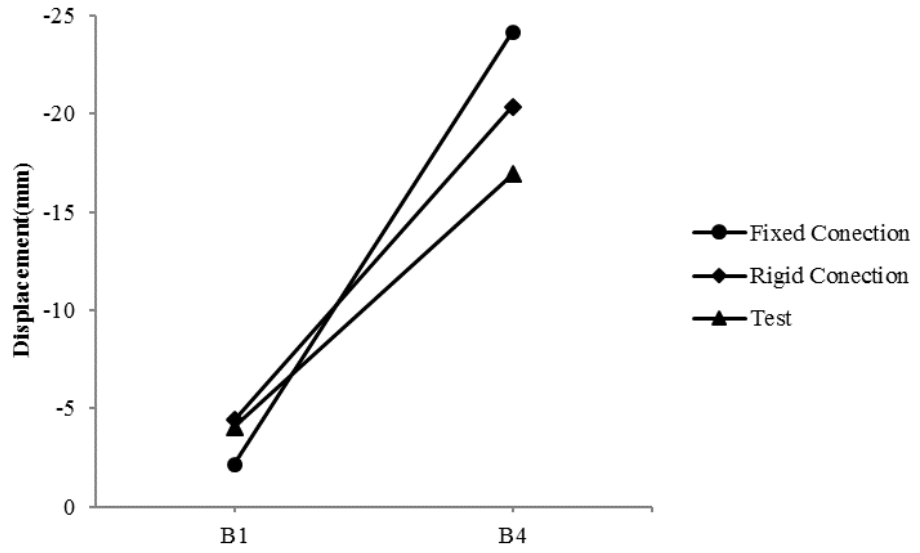

Fig. 18. Displacements of B1 and B4 middle span in static torsion test for various connections

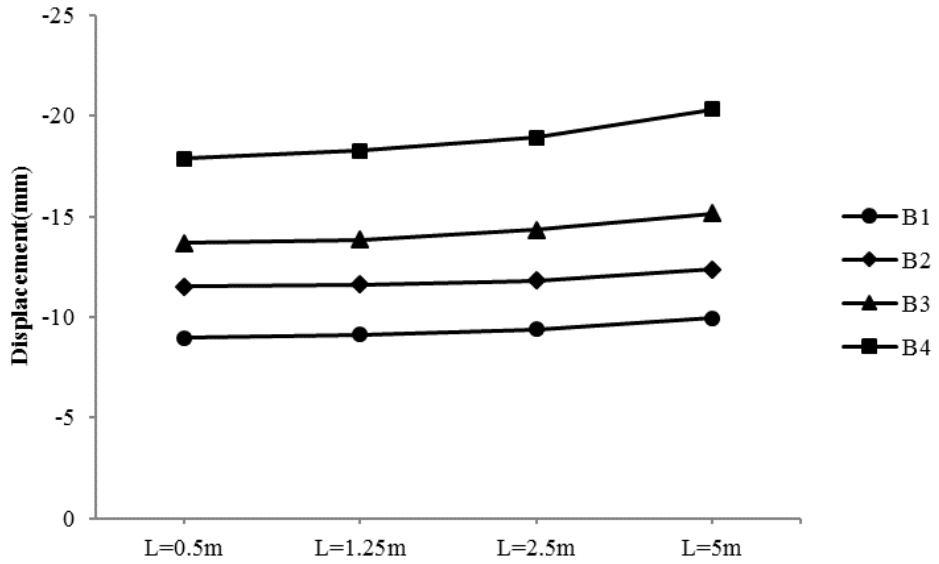

Fig. 19. Displacements of B1 to B4 middle span of the fourth section in static bending test for various spacing

As the transversal element spacing decreases the displacement results also decreases (Figure 19).

Slab Stiffness Changes

The presence of elastomeric bearings means that the slab's stiffness system is an indeterminate parameter in the model calibration procedure. This is because the performance of the devices under the applied loads is fully unknown after their service life. Also, the elastomeric bearings' lateral movement after their service life and possibility of incorrect implementation intensifies the inaccuracy (Figure 20). Slab stiffness changes in beams 3 and 4 (Figure 21).

According to the results earlier mentioned, transversal element to girder connection, transversal element spacing, and slab stiffness changes are the most effective parameters in model calibration. Table 5 shows the values of these calibration parameters of the model.

Figures 22-25 show the displacements of the calibrated model and real bridge. It can be seen that a good relationship exists between the model and test data.

Fig. 20. Elastomeric bearing of lateral movement in the Ghale Morghi bridge

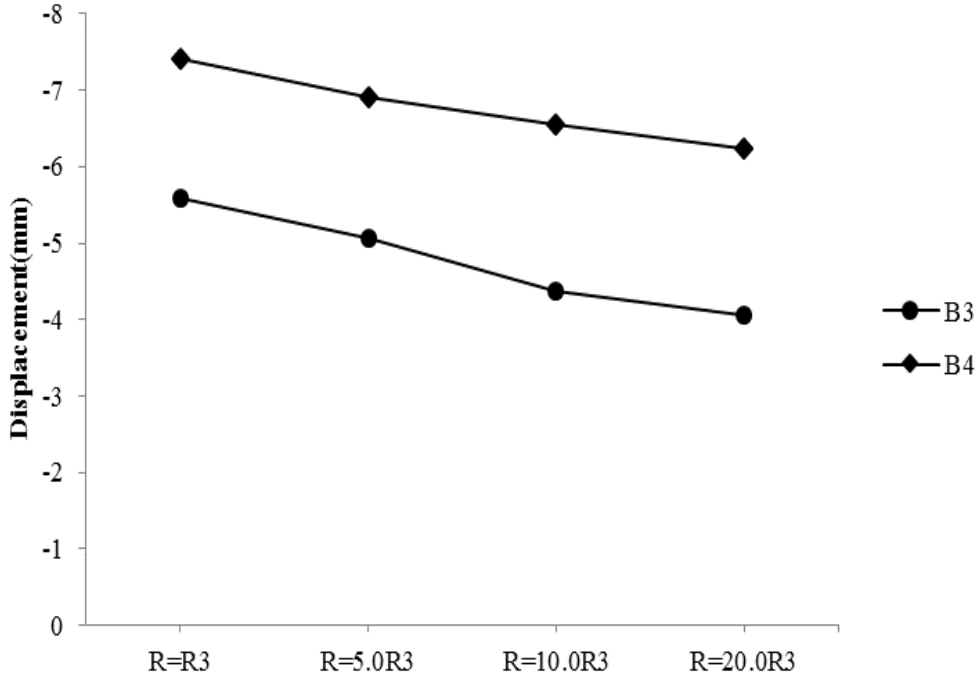

Fig. 21. Displacement of B3 and B4 middle span in static bending test for various stiffness- vehicles at the 3rd position

Table 5. Parameters of calibrated model

Model Parameter	Value or Manner
Transversal element spacing	500 mm
Elasticity Modulus of Concrete	27386 MPa
Transversal element connection to girder	rigid confection

Table 6. Bending stiffness of calibrated model in pier of R3 support under various beams

	B1	B2	B3	B4
P2	23.44×10^3	23.44×10^3	46.88×10^3	46.88×10^3
P3	22.59×10^4	22.59×10^4	22.59×10^4	45.1×10^4
P4	22.59×10^4	22.59×10^4	22.59×10^4	45.1×10^4
P5	23.44×10^3	23.44×10^3	46.88×10^3	46.88×10^3

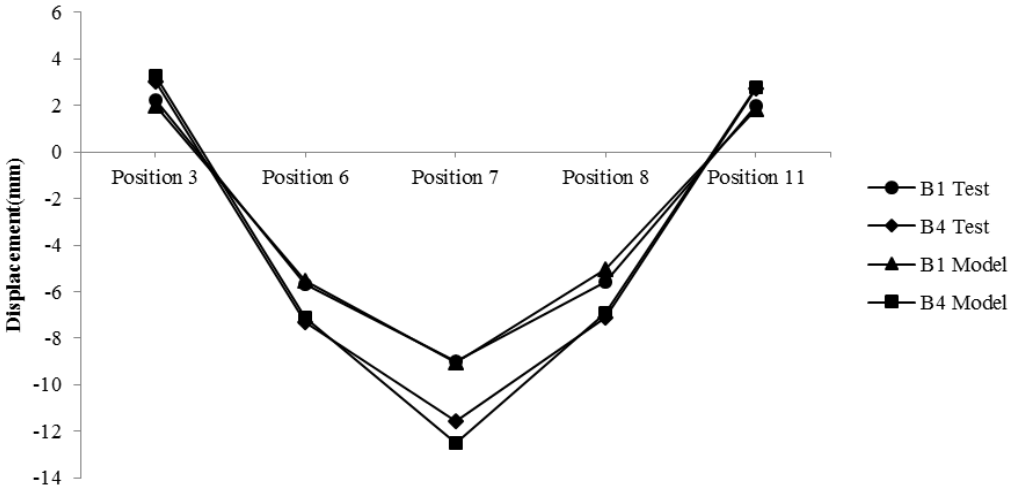

Fig. 22. Displacement of B1 and B4 in middle span of the fourth section in static bending test for various vehicle positions

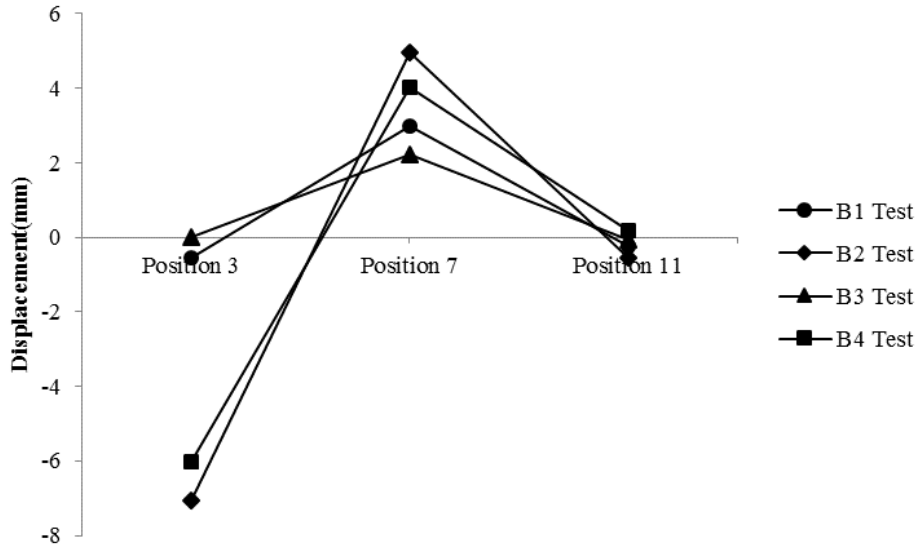

Fig. 23. Displacement of B1 and B4 in the first section of the static torsion test for various vehicle positions

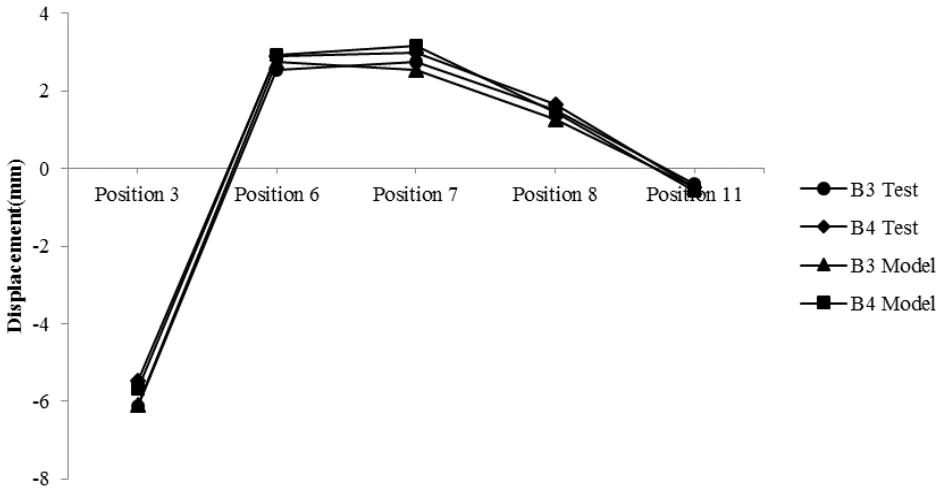

Fig. 24. Displacement of B3 and B4 in the second section of the static bending test for various vehicle positions

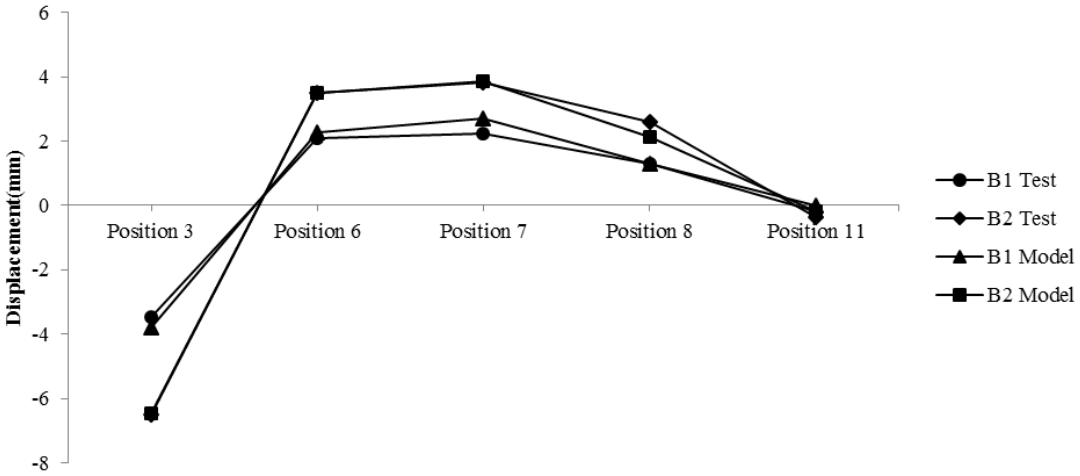

Fig. 25. Displacement of B1 and B2 in the second section of the static bending test for various vehicle positions

As can be seen from the above figures, the numerical model has a good agreement with real test results. The numerical modeling of the static bending test in different sections is in complete agreement with the corresponding experimental results as shown in Figures 24 and 25. This is not the case for torsion test results, where some discrepancy could be seen between the numerical results and those of the tests shown in Figures 22 and 23. This indicates that the deck of the numerical model twists considerably.

STRUCTURAL HEALTH

Estimating or rating the damage of bridges is an item that is of great interest in structural health monitoring as damage detection (Gomez et al., 2011; Hui et al., 2011). Considering the importance of the technical structures, their damage causes disruptions in traffic and also brings many risks. In this paper, the percentage of structural health using AASHTO code was estimated.

Step 1. Structural health of AASHTO code

Table 7 shows the AASHTO code of damage or health of structure.

Step 2. Damage weights

Since different damaged parts of the bridge are not the same and have different effects on the behavior of the bridge, it is necessary to associate them with different weights. These damage weights are determined by bridge engineering experts (Table 8).

Table 7. Range of structural health and bridge damage (AASHTO code)

Cod	Situation	Explanation of Damage	Structural Health (%)
9	excellent	without damage	90-100
8	very good	very tiny damage	80-90
7	good	smaller than 2% damage	70-80
6	satisfactory	2-10% damage	60-70
5	pretty good	10-25% damage	50-60
4	week	25-50% damage	45-50
3	dangerous	more than 50% damage	30-45
2	critical	-	25-30
1	imminent collapse	-	30-25
0	collapse	-	0-10

Table 8. Damage weight of bridge components

The Main Component of Bridge	Member Surveyed	Damages Weight of Member on Structure (%)
1. Bridge pavement	1-1- railroad pavement layer	6%
2. Deck component	2-1- expansion joint 2-2- drainage system 2-3- tables and pedestrians 2-4- concrete deck	9%
3. Super structures member	3-1- main super structures (longitudinal girders)	20%
	3-2- diaphragms	10%
	3-3- supports 3-4- lateral supports	10%
4. Substructures member	4-1- side pile of bridge	19%
	4-2- middle pile of bridge	20%
	4-3- ramp wall	6%
Total Weight		100%

Step 3. Structural health score

After bridge inspection, according to the type and extent of damage, scores were attributed to the members, and the total scores of damage of a bridge member divided by the total scores of ideal members to obtain the structural health percentage of the surveyed member (Eq. (1)) (Gomez et al., 2011; Hui et al., 2011). The number 9 is the ideal basis scores.

$$\text{A member's health (\%)} = \frac{\text{the total scores of damage of that member}}{\text{total scores of ideal member}} \quad (1)$$

In the next step, the effective weights were multiplied with the percentage of member's health, to determine its effect on the entire structure, as shown in Eq. (2), given as:

$$\text{Effect of member damage to whole structue (\%)} = \text{Damage weight of member} \times \text{Member's health} \quad (2)$$

Obviously, the ratio of the total scores of damaged members to the total scores of ideal members is the best parameter to describe structural health. Of course, despite the weight of each factor and the use of skilled and experienced opinion in determining the damage of any member and the weight of any damage in the equation, this paper will be very useful and reliable in describing health structures. Finally, considering the total damage of all members, the final health score of the bridge was evaluated as 89%, which means the bridge is in a very good situation.

SUMMARY AND CONCLUSIONS

In this paper, load testing of the Ghale Morghi bridge was investigated in order to identify the defects that cause vibration in surrounding buildings. A hundred and two (102) sensors comprised of displacement, strain and accelerator gauges were installed at the critical points. The bridge Structure was loaded statically and dynamically in two steps using six vehicles. In the primary review of the bridge, girders were not properly seated on elastomeric bearings in some cap beams. In the static load test, a low range of strains and displacements illustrated adequate structural capacity and appropriate safety under static loads. Although, the dominant frequency of vibration of the bridge (2.6 Hz) was close

to that of nearby buildings (2.5 Hz) and consequently disturbing vibrations were induced in the surrounding buildings. Anyway, causes of undesirable vibrations of the Ghale Morghi Bridge may include: 1. The presence of surface roughness, 2. natural frequency of the bridge being close to that of the nearby buildings or 3. natural frequency of the bridge being close to that of the passing vehicles.

In this research, it was shown that a properly designed scheme for installing acceleration, displacement and strain gauges at critical points of a bridge superstructure can help to investigate the behavior of the bridge under different loading conditions without having to build very accurate models and perform time-consuming non-linear analyses. It also helps to assess the adequacy of the bridge structure to sustain the loads that were exerted on it during its existence. This bridge is curved in the horizontal plane and the lack of a unifying load-resisting system in the transverse direction caused the bridge to have a torsional mode of vibration. In this paper, the model was calibrated comparing the numerical model and the load testing results. Transversal element to girder connection, transversal element spacing, and slab stiffness changes were shown to be the most influential parameters in the calibration process of the bridge. Finally, the score of the bridge's health was evaluated as 89% which means that the Ghale Morghi bridge is in a very good shape.

ACKNOWLEDGEMENTS

The Ghale Morghi bridge load test was supported by Tehran municipality in corporation with I.R of Iran railways. The authors would like to acknowledge the support.

REFERENCES

AASHTO Standard Specification for Highway Bridges. (2002). 17th ed., American Association of State Highway and Transportation Officials. 444 North Capitol Street, N.W., Suite 249 Washington, D.C. 20001, ISBN: 156051-171-0.

AASHTO guide specifications for horizontally curved steel girder highway bridges with design examples for I-girder and Box-girder bridges. (2003). American Association of State and Highway Transportation Officials. By ballot of the AASHTO Highway Subcommittee on Bridges and Structures (HSCOBS).

Adewuyi, A.P. and Wu, Z.S. (2009). "Vibration-Based structural health monitoring techniques using statistical features from strain measurements", *ARPN Journal of Engineering and Applied Sciences*, 4(3), 38-47.

Ataeia, S., Aghakouchaka, A.A., Marefatb, M.S. and Mohammadzadeh, S. (2005). "Sensor fusion of a railway bridge load test using neural networks", *Expert Systems with Applications*, 29(3), 678-683.

Chang, C.J. and White, D.W. (2008). "An assessment of modeling strategies for composite curved steel I-girder bridges", *Engineering Structures*, 30(11), 2991-3002.

Darius, B., Zenonas, K., Donatas, J. and Arturas, K. (2013). "Load testing and model updating of a single span composite steel-concrete railway", *Procedia Engineering*, 57, 127-135.

Demetrios, E. and Tonias, P.E. (1995). *Bridge engineering*, New York: McGraw-Hill, New York.

Ghorbanpour, A.H. and Ghassemieh, M. (2011). "Vertical vibration of composite floor by neural network analysis", *Civil Engineering Infrastructures Journal*, 42(1), 117-126.

Gomez, H.C., Fanning, P.J., Fenga, M.Q. and Lee, S. (2011). "Testing and long-term monitoring of a curved concrete box girder bridge", *Engineering Structures*, 33(10), 2861-2869.

Green, M.F. and Cebon, D. (1994). "Dynamic response of highway bridges to heavy vehicle loads: Theory and experimental validation", *Journal of Sound Vibration*, 170(1), 51-78.

Hui, L., Shujin, L., Jinping, O., Xuefeng, Z., Wensong, Z., Yan, Y., Na, L. and Zhiqiang, L. (2011). "Investigation of vortex-induced vibration of a suspension bridge with two separated steel box-girders based on field measurements", *Engineering Structures*, 33(6), 1894-1907.

Ilze, P. and Ainars, P. (2013). "The dynamic amplification factor of the bridges in Latvia", *Procedia Engineering*, 57, 851-858.

Kavatani, M., Kobayashi, Y. and Kawaki, H. (2000). "Influence of elastomeric bearings on traffic-induced vibration of highway bridges", *TRR National Research Council*, 1696(1), 76-82.

Kistera, G., Wintera, D., Badcocka, R.A., Gebremichaelb, Y.M., Boyleb, W.J.O., Meggittc, B.T., Grattanb, K.T.V. and Fernandod, G.F.

(2007). "Structural health monitoring of a composite bridge using Bragg grating sensors. Part 1: Evaluation of adhesives and protection systems for the optical sensors", *Engineering Structures*, 29(3), 440-448.

Kwak, H.G., Seo, Y.J. and Jung, C.M. (2000). "Effects of the slab casting sequences and the drying shrinkage of concrete slabs on the short-term and long-term behavior of composite steel box-girder bridges", *Engineering Structure*, 22(11), 1453-1466.

McCullagh, J.J., Galchev, T., Peterson, R.L., Gordenker, R., Zhang, Y., Lynch, J. and Najafi, K. (2014). "Long-term testing of a vibration harvesting system for the structural health monitoring of bridges*", Sensors and Actuators A: Physical*, 217, 139-150.

Mohammad, S.M., Gargary, E.G. and Ataei, S. (2004). "Load test of a plain concrete arch railway bridge of 20-m span", *Construction and Building Materials*, 18(9), 661-667.

Montens, M., Vollery, C. and Park, H. (2003). "Advantages of twin I beams composite solutions for highway and railway bridges", *Steel Structures International Journal*, 3(1), 65-72.

Naeeni, S.T.O., and Fazli, M. (2011). "Numerical investigation of effect of bridge pier shape on dynamic forces", *Civil Engineering Infrastructures Journal*, 44(5), 741-751.

Office of the Deputy for Technical Affairs Bureau of Technical Affairs and Standards of I.R of Iran. (2000). Standard loads for bridges, No.139, Tehran, Iran

Scott, D.S., Joseph, J.P., Christopher, M.I. and Kevin, J.A. (2006). "Load testing for assessment and rating of highway bridges, Phase III: Technology transfer to the SCDOT", *South Carolina Department of Transportation Research and Development Executive Committee*. Research Project No. 655. United States. Federal Highway Administration. Clemson University Civil Engineering Department.

Sevim, B., Bayraktar, A., Altunisik, A.C., Atamturktur, S. and Birinci, F. (2011). "Finite element model calibration effects on the earthquake response of masonry arch bridges", *Finite Elements in Analysis and Design*, 47(7), 621-634.

Sun, J.K., Ho, K.K, Radiance, C., Jin, P., Gyu, S.K. and Deok, K.L. (2013). "Operational field monitoring of interactive vortex-induced vibrations between two parallel cable-stayed", *Journal of Wind Engineering and Industrial Aerodynamics*, 123(Part A), 143-154.

Wang, H., Li, A.Q. and Li, J. (2010). "Progressive finite element model calibration of a long-span suspension bridge based on ambient vibration and static measurements", *Engineering Structures*, 32(9), 2546-2556.

Yang, Y.B., Lin, C.L., Yau, J.D. and Chang, D.W. (2004). "Mechanism of resonance and cancellation for train-induced vibrations on bridges with elastic bearings", *Journal of Sound Vibration*, 269(1-2), 345-360.

Yarnold, M.T. and Moon, F.L. (2015). "Temperature-based structural health monitoring baseline for long-span bridges", *Engineering Structures*, 86, 157-167.

Yau, J.D., Wu, Y.S. and Yang, Y.B. (2001). "Impact response of bridges with elastic bearings to moving loads", *Journal of Sound and Vibration*, 248(1), 9-30.